RESEARCH ARTICLE

Disease Models & Mechanisms 3, 236-245 (2010) doi:10.1242/dmm.003772

Predominant cone photoreceptor dysfunction in a hyperglycaemic model of non-proliferative diabetic retinopathy

Yolanda Alvarez[1,*], Kenneth Chen[1], Alison L. Reynolds[1], Nora Waghorne[1], John J. O'Connor[1] and Breandán N. Kennedy[1,*]

SUMMARY

Approximately 2.5 million people worldwide are clinically blind because of diabetic retinopathy. In the non-proliferative stage, the pathophysiology of this ocular manifestation of diabetes presents as morphological and functional disruption of the retinal vasculature, and dysfunction of retinal neurons. However, it is uncertain whether the vascular and neuronal changes are interdependent or independent events. In addition, the identity of the retinal neurons that are most susceptible to the hyperglycaemia associated with diabetes is unclear. Here, we characterise a novel model of non-proliferative diabetic retinopathy in adult zebrafish, in which the zebrafish were subjected to oscillating hyperglycaemia for 30 days. Visual function is diminished in hyperglycaemic fish. Significantly, hyperglycaemia disrupts cone photoreceptor neurons the most, as evidenced by prominent morphological degeneration and dysfunctional cone-mediated electroretinograms. Disturbances in the morphological integrity of the blood-retinal barrier were also evident. However, we demonstrate that these early vascular changes are not sufficient to induce cone photoreceptor dysfunction, suggesting that the vascular and neuronal complications in diabetic retinopathy can arise independently. Current treatments for diabetic retinopathy target the vascular complications. Our data suggest that cone photoreceptor dysfunction is a clinical hallmark of diabetic retinopathy and that the debilitating blindness associated with diabetic retinopathy may be halted by neuroprotection of cones.

INTRODUCTION

Diabetic retinopathy (DR) is the leading cause of blindness for working-age individuals in developed countries (Wong et al., 2006; Morello, 2007). Diabetes afflicts ~170 million individuals worldwide, with ~78-98% progressing to DR within 15 years of diagnosis. DR is divided into initial non-proliferative DR (NPDR) and subsequent proliferative DR (PDR) stages, reflecting the inappropriate growth of new leaky blood vessels in the later stage. DR pathology stems from the hyperglycaemia associated with diabetes. Elevated blood glucose levels can modify metabolic processes owing to the overproduction of superoxide in the mitochondrial electron-transport chain (Brownlee, 2001). This can increase the production of advanced glycation end products (AGE) and the accumulation of free radicals that activate inflammatory mechanisms (Brownlee, 2001; Hernandez and Simo, 2007).

DR is a dual disorder that includes microvascular complications and neurodegeneration of the retina (Gardner et al., 2002; Simo et al., 2006). Vascular changes in NPDR include retinal capillaries with disrupted cell-cell junctions, thickened basement membranes and loss of pericytes (Garner, 1970; Simo et al., 2006; Frank, 2009). In addition, vessels become leaky and acellular, circulation is compromised and retinal oedema appears owing to plasma extravasation from the capillaries (Greenstein et al., 2000; Frank, 2004). All of these vascular changes lead to a breakdown of the blood-retinal barrier and compromise retinal function. In NPDR, damaged endothelial cells synthesise vasoconstrictors, retinal capillaries become thrombogenic, and archetypical 'cotton wool spots' appear, which are indicative of retinal ischemia (Frank, 2004; Simo et al., 2006).

Retinal ischemia usually progresses to severe hypoxia, triggering PDR characterized by neovascularisation (Garner, 1970; Simo et al., 2006). In response to retinopathic hypoxia, angiogenic factors including vascular endothelial growth factor (VEGF) are secreted and new blood vessels grow inappropriately into the vitreous (Frank, 2004; Hernandez and Simo, 2007). These new vessels are fragile, leading to extensive intraocular haemorrhaging. Additionally, the vessels anchor to the vitreous via fibrous tissue that is prone to contraction, producing tension on the retina and eventually causing retinal detachment and blindness (Gardner et al., 2002; Frank, 2004).

Interest in the neuropathological aspect of DR has been revived recently (Cho et al., 2000; Gardner et al., 2002; Simo et al., 2006). The functional loss of retinal neurons in diabetics was described five decades ago (Wolter, 1961), and DR patients commonly fail colour vision and contrast sensitivity tests (Daley et al., 1987). In fact, in diabetics, abnormal visual function, as assessed by electroretinography (ERG), usually precedes the clinical onset of retinal neovascularisation (Bresnick and Palta, 1987; Juen and Kieselbach, 1990; Yamamoto et al., 1996; Parisi and Uccioli, 2001; Gardner et al., 2002).

To date, the specific cell types undergoing neuropathology in the retinas of diabetics have not been clearly identified, with contradictory results in post-mortem analyses (Wolter, 1961; Barber et al., 1998; Cho et al., 2000; Carrasco et al., 2007; Carrasco et al., 2008). Recently, it has become apparent that, in DR, retinal neurodegeneration occurs prior to retinal neovascularisation. However, it is unclear whether the early vascular changes and the retinal neuropathology develop independently.

[1]UCD School of Biomolecular and Biomedical Sciences, UCD Conway Institute, University College Dublin, Belfield, Dublin D4, Ireland
*Authors for correspondence (yolanda.alvarez@ucd.ie; brendan.kennedy@ucd.ie)

Current treatments for DR target the vasculature, stunting the inappropriate growth of new blood vessels during late-stage PDR. Laser photocoagulation is a surgical approach that ablates unwanted vessels, but also adjacent healthy tissue. Although this intervention can halt PDR progression, it is a palliative therapy for advanced disease (Wilkinson-Berka and Miller, 2008). In addition, success is partial and associated with serious side effects including visual field loss, recurrent vitreal haemorrhage, cataracts and retinal detachment (Hernandez and Simo, 2007; Wilkinson-Berka and Miller, 2008). Molecular therapies in clinical trials block retinal neovascularisation using antibodies, small interfering RNAs (siRNAs) or small molecule inhibitors targeted to pro-angiogenic pathways (Campochiaro, 2007; Wilkinson-Berka and Miller, 2008; Frank, 2009). By contrast, no DR therapies target the earlier NPDR stage, nor do they aim to protect the endangered retinal neurons. Thus, comprehension of the neuronal and vascular abnormalities in the initial phases of NPDR may reveal therapeutic targets that more effectively block disease progression.

Numerous animal models of DR have been proposed, and although some phenocopy certain diabetic complications well, none is without limitations (see www.amdcc.org). To our knowledge, there is no animal model that recapitulates all of the neural and vascular complications that are associated with NPDR and PDR in humans. Strategies to induce DR include the destruction of beta cells in the pancreas by surgical removal or drug treatment with streptozotocin (STZ) (Rees and Alcolado, 2005). STZ, which is probably the most widely used compound to model type 1 diabetes, is a glucosamine-nitrosourea derivate and is very efficient in destroying pancreatic beta cells, but its toxicity and carcinogenicity produce unwanted side effects (Rees and Alcolado, 2005; van Eeden et al., 2006) In modelling DR, STZ treatment induces transient apoptosis in the neuroretina, glial activation, impaired electroretinograms (ERGs) and some hallmarks of early microangiopathy including open blood-retinal barriers. The phenotypes induced have a late developmental onset and do not progress to PDR (Barber et al., 1998; Zeng et al., 2000; Li et al., 2002; Park et al., 2003; Feit-Leichman et al., 2005).

Inbred rodent strains selected for hyperglycaemia include the non-obese diabetic mouse (NOD), the bio-breeding rat (BB) and the Goto-Kakisaki rat (GK) (Nakhooda et al., 1977; Makino et al., 1980). Although these models identify genetic determinants of diabetes, their application to DR research is limited owing to their reduced life span (Portha et al., 2001; Rees and Alcolado, 2005). Transgenic mice overexpressing VEGF or insulin-like growth factor (IGF) in the retina indirectly model PDR by inducing neovascularisation and retinal detachment (Ruberte et al., 2004; Shen et al., 2006; van Eeden et al., 2006); however, these models can precipitate developmental defects, may disrupt the cells expressing the transgene and, importantly, they bypass growth factor-independent pathologies arising from hyperglycaemia. In this regard, exposure to high concentrations of glucose is widely used for cell culture models of diabetes (Haselton et al., 1998; Mandal et al., 2006; Fraser et al., 2007; Ihnat et al., 2007) but fails to induce DR phenotypes in wild-type rodents (www.amdcc.org) (Rees and Alcolado, 2005).

Zebrafish have excellent potential for diabetes research (Kinkel and Prince, 2009). A simple method to induce sustained hyperglycaemia in zebrafish was described recently by Gleeson et al. (Gleeson et al., 2007). Alternating between 24 hours of glucose treatment and 24 hours of rest in system water for 30 days induces high blood glucose levels in adult zebrafish. The authors also reported a reduction in the thickness of the retinal inner plexiform layer but did not address vascular changes in the retina (Gleeson et al., 2007). The inner retina of zebrafish was also recently demonstrated to be nourished by an intricate vascular network that shares many features with the human hyaloid and retinal vasculatures (Alvarez et al., 2007). Thus, we investigated whether the retinas of hyperglycaemic zebrafish recapitulate the morphological and/or functional changes that are associated with early-stage human NPDR.

Here, we demonstrate that the retinas of hyperglycaemic zebrafish display neurodegenerative and vascular hallmarks of early-stage NPDR. Retinal capillaries have thickened basement membranes and compromised blood-retinal barrier architecture. Significantly, we observe a unique susceptibility of cone photoreceptors to hyperglycaemia, which was revealed by extensive degeneration of cone cell morphology and defective photopic ERGs. Finally, our data demonstrate that the cone dysfunction and morphological degeneration induced by hyperglycaemia develop independent of the early vascular pathologies that are induced by hyperosmolarity.

RESULTS

Hyperglycaemia causes thickening of retinal vessels

One- and 2-year-old adult zebrafish were treated with 2% glucose (~110 mM) to induce hyperglycaemia, as described previously (Gleeson et al., 2007). After 30 days, glucose-treated fish show no apparent abnormalities in their overall morphology or behaviour. Control fish that were kept in system water during the treatment period were slightly thinner. By contrast, retinal vessels from 2-year-old hyperglycaemic fish were visibly thicker than age-matched controls, especially at locations proximal to the central optic disc (Fig. 1C,D,F). Although thicker retinal vessels were apparent, no difference was observed in the overall patterning or number of retinal vessels compared with controls (Fig. 1A,B,E).

Hyperglycaemia destabilises the blood-retinal barrier and leads to basement membrane thickening

For all subsequent treatments, mannitol-treated fish were included as a hyperosmolarity control. To evaluate the effects of hyperglycaemia on the ultrastructure of the blood-retinal barrier, vessels from control, glucose-treated and mannitol-treated retinas were analysed by transmission electron microscopy (TEM) (Fig. 2). Both tight (TJ) and adherent (AJ) interendothelial junctions were significantly wider in the retinal vessels of all fish subjected to glucose or mannitol compared with water controls (Fig. 2A,C). This morphological disruption of the blood-retinal barrier architecture suggests increased vessel permeability (Vinores et al., 1992). As this early vascular phenotype was observed after glucose or mannitol treatment, it is a feature of hyperosmolarity and is not unique to hyperglycaemia. Notably, the vessel basement membrane is significantly thicker in glucose-treated fish, but not in mannitol-treated or control fish (Fig. 2B,D). Thickening of the basement membrane in retinal capillaries is the first and most widely accepted hallmark of DR (Garner, 1970; Wilkinson-Berka and Miller, 2008).

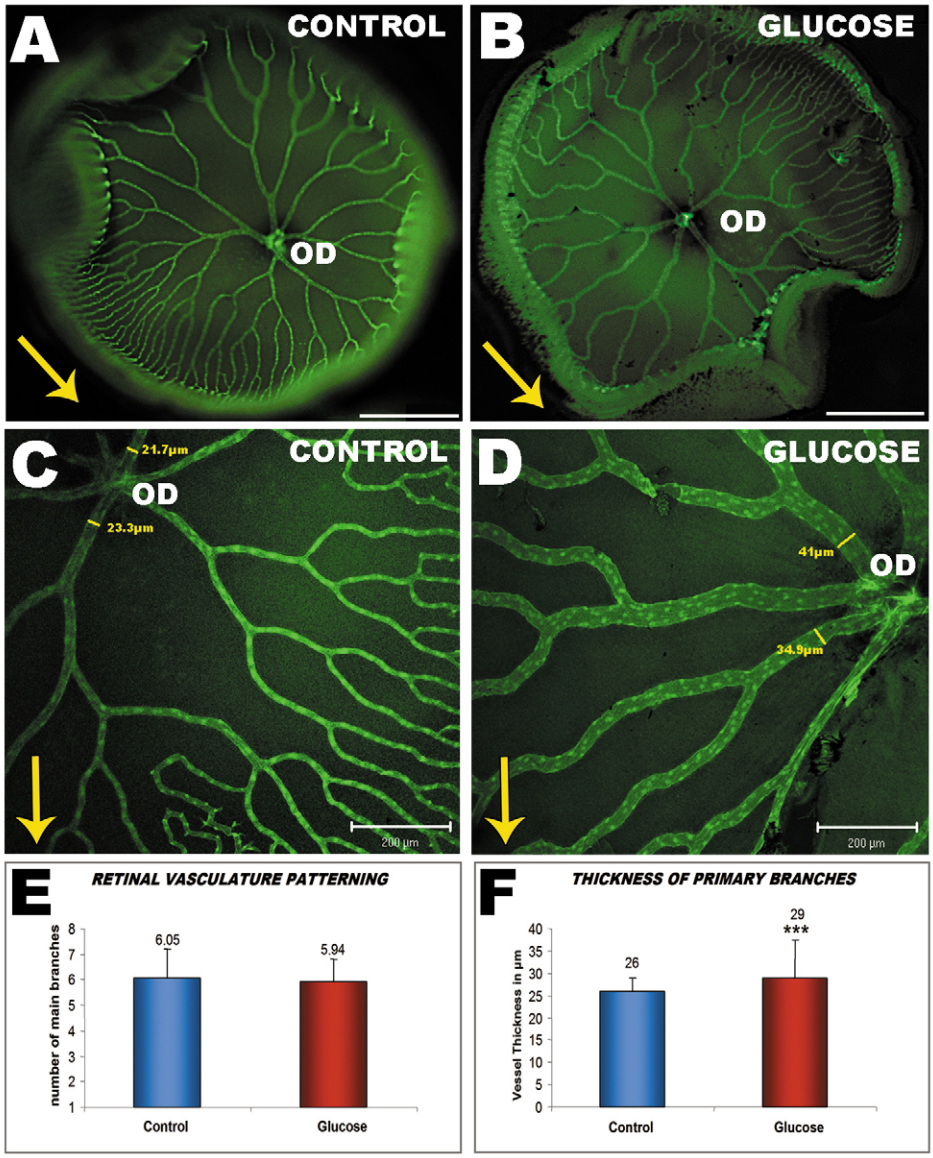

Fig. 1. Hyperglycaemia affects the thickness but not the patterning of the retinal vessels in 2-year-old zebrafish. (A) Overall morphology of the retinal vessels in a control 2-year-old zebrafish displaying the archetypal vascular arrangement, with 5-9 main branches (six in the image shown) radiating from the optic disc (OD) and covering the whole inner retina surface. (B) In glucose-treated, 2-year-old fish, the general structure of the retinal vascular network does not differ from the controls (six main branches in the retina shown). (C) Confocal image of the flat-mounted central retina of a control zebrafish showing that the main branches at locations proximal to the optic disc exhibit a standard thickness (~26 µm). (D) Confocal image of the flat-mounted central retina of a hyperglycaemic fish showing thickened retinal vessels, especially in the central retina (up to 45 µm). (E) The number of main branches radiating from the optic disc is identical in control and glucose-treated fish (control fish, *n*=29; glucose-treated fish, *n*=16). (F) Graph of the thickness of retinal vessels at locations proximal to the optic disc (control fish, *n*=5; glucose-treated fish, *n*=9). Retinal vessels were significantly thicker in hyperglycaemic fish (***P<0.001). The error bars in E and F show the standard error of the mean (S.E.M.). Yellow arrows indicate the dorso-ventral axis in the whole-mount retinas. Bars, 500 µm (A,B); 200 µm (C,D).

Using reverse transcription (RT)-PCR, we observed a sharp upregulation of $VEGF_{165}$ in glucose- and mannitol-treated fish (Fig. 2E). This is in agreement with the increased VEGF levels in DR (Sone et al., 1997; Frank, 2004), especially of the $VEGF_{165}$ isoform that has been linked with pathological angiogenesis (Simo and Hernandez, 2008). By contrast, no significant differences in the expression levels of tight junction protein 1 (TJP1) (ZO-1 in humans), cone transducin alpha (Tc-α) or β-actin were observed (Fig. 2E).

Hyperglycaemia induces adult retinal degeneration

Retinal sections of control, glucose-treated and mannitol-treated fish were analysed to evaluate retinal cell integrity (Fig. 3). Light microscopy analyses revealed no significant difference in the thickness of the retina or any retinal sublayer (Fig. 3, and data not shown). Furthermore, the histology of control and mannitol-treated retinas were normal and indistinguishable (Fig. 3A,A',D,D'). However, TUNEL (TdT-mediated dUTP nick-end labelling) analysis of retinal cryosections revealed high levels of apoptosis in mannitol-treated retinas, especially in the vascular and ganglion cells (supplementary material Fig. S1). Hyperglycaemia, which also results in hyperosmolarity, does not induce ganglion cell layer (GCL) apoptosis, perhaps because hyperglycaemia induces expression of the anti-apoptotic factor Bcl2 (Pampfer et al., 2001; Fraser et al., 2007).

By stark contrast, light microscopy revealed that ~60% of glucose-treated fish displayed abnormal retinal histology with prominent defects in cone photoreceptors (Fig. 3B,B',C,C'). In approximately half of these retinas, hyperglycaemia caused severe morphological defects with pronounced signs of cone photoreceptor degeneration (Fig. 3B,B'). Some pyknotic nuclei were detected in the outer nuclear layer of the fish that were severely affected by the glucose treatment (black arrows in Fig. 3B), although the levels of apoptosis, measured by TUNEL, on retinal cryosections were not increased compared with controls (supplementary material Fig. S1). Necrotic traits observed in the

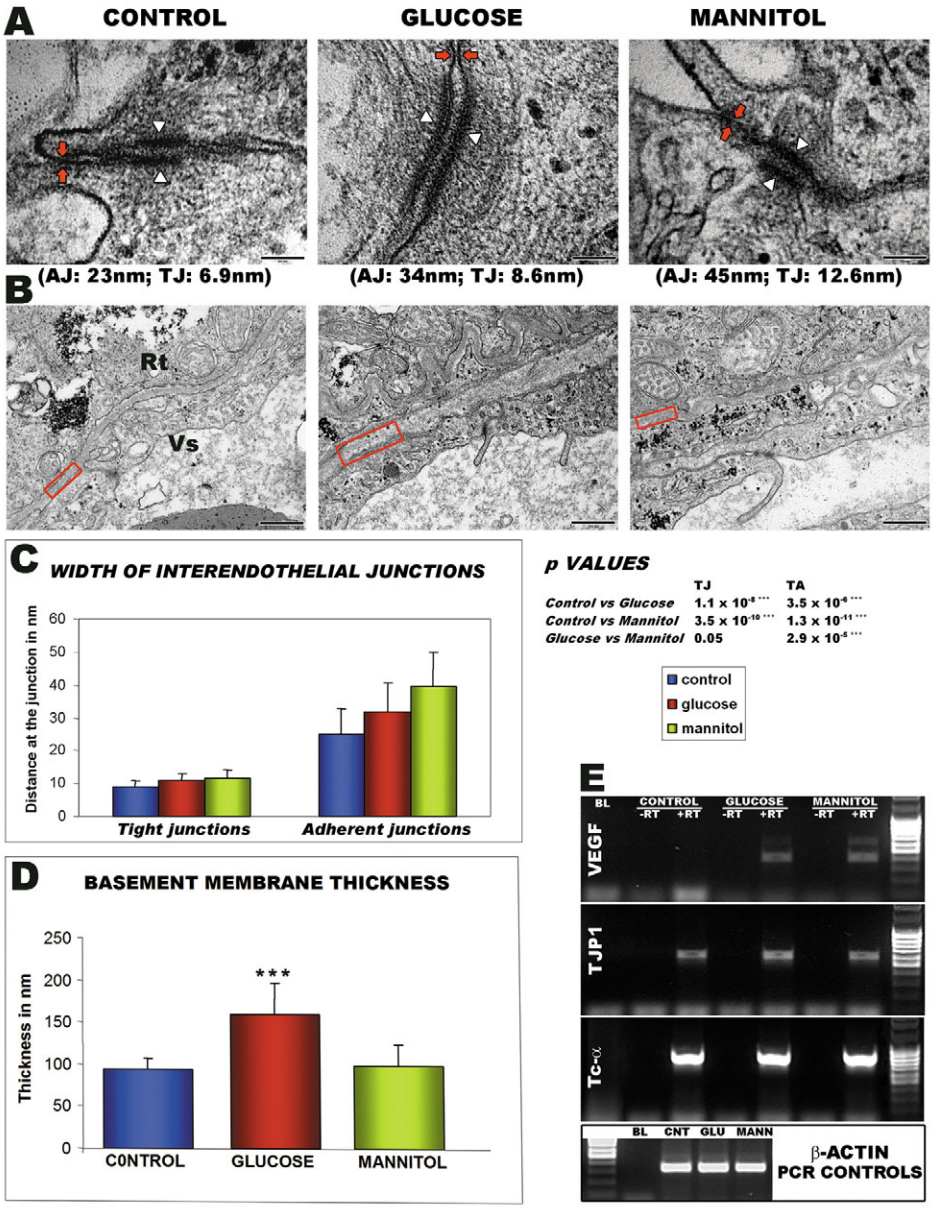

Fig. 2. The retinal blood barrier is compromised in glucose- and mannitol-treated fish. (A) Representative TEM images of interendothelial junctional complexes in vessels at central locations of the retina from control, glucose-treated and mannitol-treated fish. The location of the tight junctions (TJ) and adherent junctions (AJ) are indicated by red arrows and white arrowheads, respectively. Bars, 100 nm. (B) Representative TEM images of the basement membrane in the retinal capillaries at central locations of the retina from control, glucose-treated and mannitol-treated fish. The retinal side (Rt) is located on top and the vascular side (Vs) is at the bottom. A red square on the left of each image depicts a portion of the basement membrane. Bars, 500 nm. (C) TJ and AJ widths (the distance between the two endothelial cells at the junction) measured at central retinal locations ($n \geq 7$ measurements per retina) (retinas: control, $n=4$; glucose treated, $n=10$; mannitol treated, $n=6$). Both the TJs and AJs were significantly wider in glucose- and mannitol-treated zebrafish than in controls (error bars: S.E.M.; *P* values are shown at the right side of the graph). (D) Basement membrane thickness of the retinal vessels measured at three central locations in each retina (retinas: control, $n=4$; glucose treated, $n=10$; mannitol treated, $n=6$). The basement membrane is significantly thickened in glucose-treated eyes, but not in mannitol-treated or control eyes (***$P<0.001$; error bars: S.E.M.). (E) Elevated $VEGF_{165}$ expression in glucose- and mannitol-treated fish detected by RT-PCR. No changes in the expression levels of Tc-α, TJP1 or β–actin were detected in comparisons of control, glucose-treated and mannitol-treated fish.

severely affected retinas included cell swelling, tissue vacuolation (red arrows in Fig. 3B) and discontinuities in the plasma membrane (red arrows in Fig. 6B). Thus, necrosis, and not apoptosis, is likely to be responsible for the degenerating cell morphology that was observed in glucose-treated retinas.

Cone photoreceptors are affected most by hyperglycaemia

To determine whether hyperglycaemia affects the expression of cell type-specific markers in the retina, cryosections were stained by immunohistochemistry (Figs 4, 5 and supplementary material Fig. S2). Staining of ganglion cells with zn5 (Fig. 4A) and amacrine cells for parvalbumin (Fig. 4F) resulted in no significant differences between control, glucose-treated or mannitol-treated fish. Müller glia span almost the entire zebrafish retina and directly contact the retinal vessels at the GCL. In mannitol-treated retinas, glial fibrillary acidic protein (GFAP) labelling of the Müller glia revealed more intense staining, particularly in the end-feet, suggesting glial activation (Fig. 4D,E). In agreement with the light microscopy defects (Fig. 3), cone photoreceptor immunolabelling was aberrant in the glucose-treated retinas (Fig. 4B; Fig. 5). Comprehensive analysis of the individual cone subtypes [ultraviolet (UV), blue and double cones] revealed that all subtypes had less intense labelling following hyperglycaemia (Fig. 5 and supplementary material Fig. S2). However, double cones (stained with zpr1) were the most obviously affected, exhibiting discontinuous labelling and an irregular stubby-shaped cone morphology (Fig. 4B; Fig. 5A and supplementary material Fig. S2C). Staining of the rod outer segments revealed no significant difference between glucose-treated, mannitol-treated or control retinas, although milder defects cannot be excluded, as the zpr3 antibody does not depict individual cell morphology.

Hyperglycaemia results in impaired cone ERGs

To determine whether the morphological abnormalities induced by hyperglycaemia correlate with defects in visual function, ex vivo ERGs were conducted on one eye, and retinal histology examined in the contra-lateral eye (Fig. 6). The ERG records electrical activity from the outer retina in response to flashes of light. Under photopic (light-adapted) settings, the b- and d-wave amplitudes of glucose-treated fish were reduced compared with control or mannitol-treated fish (Fig. 6C-E). The reductions in the b- and d-waves were consistent with diminished signal initiation in ON and OFF bipolar cells, respectively; most likely reflecting perturbed upstream photoreceptors. In agreement, severe morphological defects were observed in the cone photoreceptors of hyperglycaemic fish (Fig. 3). Indeed, the ultrastructure of the retinas from fish with the most diminished ERGs had acute signs of cone neurodegeneration, including abnormal squat cell morphology, deteriorated mitochondria and disrupted outer segments (Fig. 6B). Vacuolations and plasma membrane discontinuities in these hyperglycaemic cones support neurodegeneration by necrosis (Fig. 6B). In agreement with the immunohistochemistry, cone but not rod photoreceptors are particularly sensitive to hyperglycaemia (Fig. 6B).

DISCUSSION

DR is a prevalent disease that results in progressive blindness. Here, we describe novel pathological features, in particular dysfunctional cones, in a zebrafish model of adult-onset DR that was confirmed by histology, immunohistochemistry, ultrastructure and electroretinography.

Hyperglycaemic treatment results in a thickening of the vessels on the surface of the zebrafish retina, a breakdown of the tightness of interendothelial cell-cell junctions, and a thickening of the vessel basement membrane. No evidence of retinal neovascularisation or significant pericyte loss was observed following the short 30-day treatment. Overall, this data is consistent with archetypal features of early-stage NPDR (Garner, 1970; Gardner et al., 2002; Hernandez and Simo, 2007; Wilkinson-Berka and Miller, 2008) and validates the hyperglycaemic zebrafish as an effective model of DR.

The most striking and most novel phenotype observed was the prevalent cone photoreceptor dysfunction and morphological degeneration in 2-year-old fish. Abnormal cone histology and severe degeneration of cone morphology were apparent in ~60% and ~30%, respectively, of the glucose-treated retinas. This variability in penetrance and severity is consistent with the unequal susceptibility of diabetics to develop retinopathy (Brownlee, 2001; Wong et al., 2006). Preliminary data also suggest that the neurodegeneration is age-dependent. Younger fish (1-year old) exposed to hyperglycaemia display more open interendothelial junctions but no evidence of neurodegeneration (supplementary material Fig. S3). This is in agreement with epidemiological studies wherein the severity of DR in humans is related to a longer duration of diabetes and a younger age of diagnosis (Klein et al., 1984; Wong et al., 2006). Rod but not cone photoreceptor perturbations have been reported in some rodent models of DR (Li et al., 2002; Park et al., 2003; van Eeden et al., 2006). In transgenic mice overexpressing $VEGF_{165}$, significant thinning of the outer nuclear and inner plexiform layers was observed at postnatal day (P)28 (van Eeden et al., 2006). Conflicting results have been reported for STZ-treated retinas: in rats, dominant photoreceptor degeneration occurs, whereas in mice, GCL apoptosis was observed (Park et al., 2003; Martin et al., 2004). In our zebrafish DR model, we observe

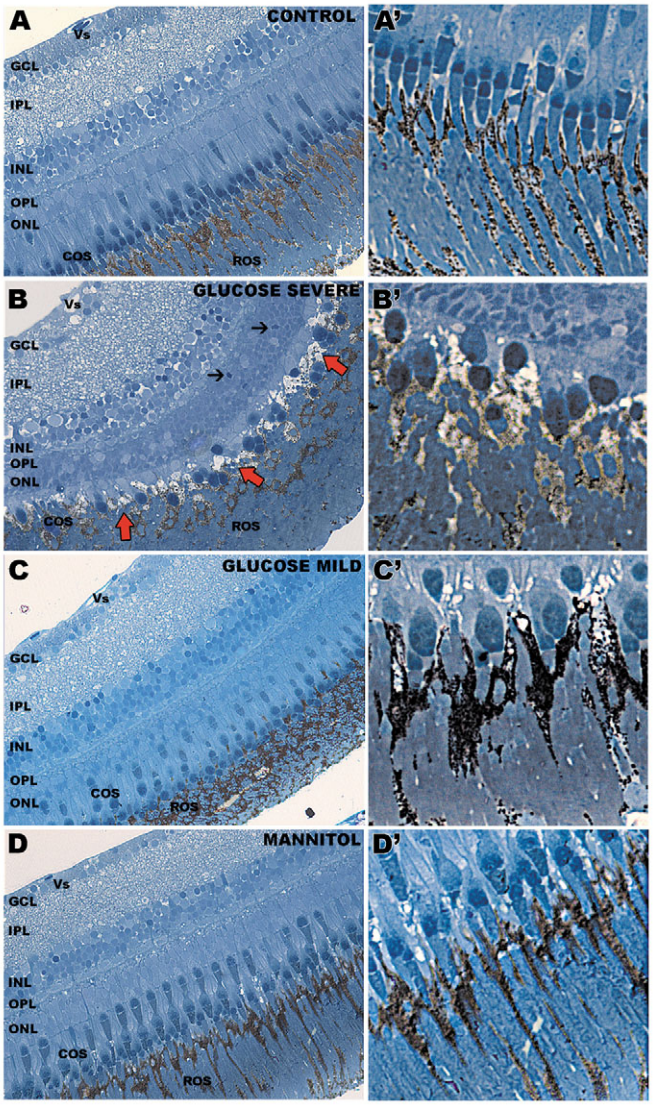

Fig. 3. Neurodegeneration is observed in glucose-treated fish. (A,A′) Light microscopy images of a histological section from a control retina showing the normal structure of the different retinal layers. (B,B′) Histological retinal sections of glucose-treated fish displaying severe photoreceptor degeneration. Sparse pyknotic nuclei (black arrows) and necrotic signs including cell swelling and tissue vacuolation (red block arrows) were observed. (C,C′) Histological retinal sections of glucose-treated fish displaying only mild abnormalities in the photoreceptor layer. (D,D′) The retinal histology in mannitol-treated fish was indistinguishable from control specimens. All images were taken of 1 µm sections from central retinal locations stained with Toluidine Blue (A-D, magnification 400×). (A′-D′) Detail of the photoreceptor histology at higher magnification (1000×). GCL, ganglion cell layer; IPL, inner plexiform layer; OPL, outer plexiform layer; INL, inner nuclear layer; ONL, outer nuclear layer; COS, cone outer segments; ROS, rod outer segments; Vs, vessel. The dark colour on the ROS area corresponds to the retinal pigmented epithelium. Retinas: *n*=10, control; *n*=15, glucose treated; *n*=13, mannitol treated.

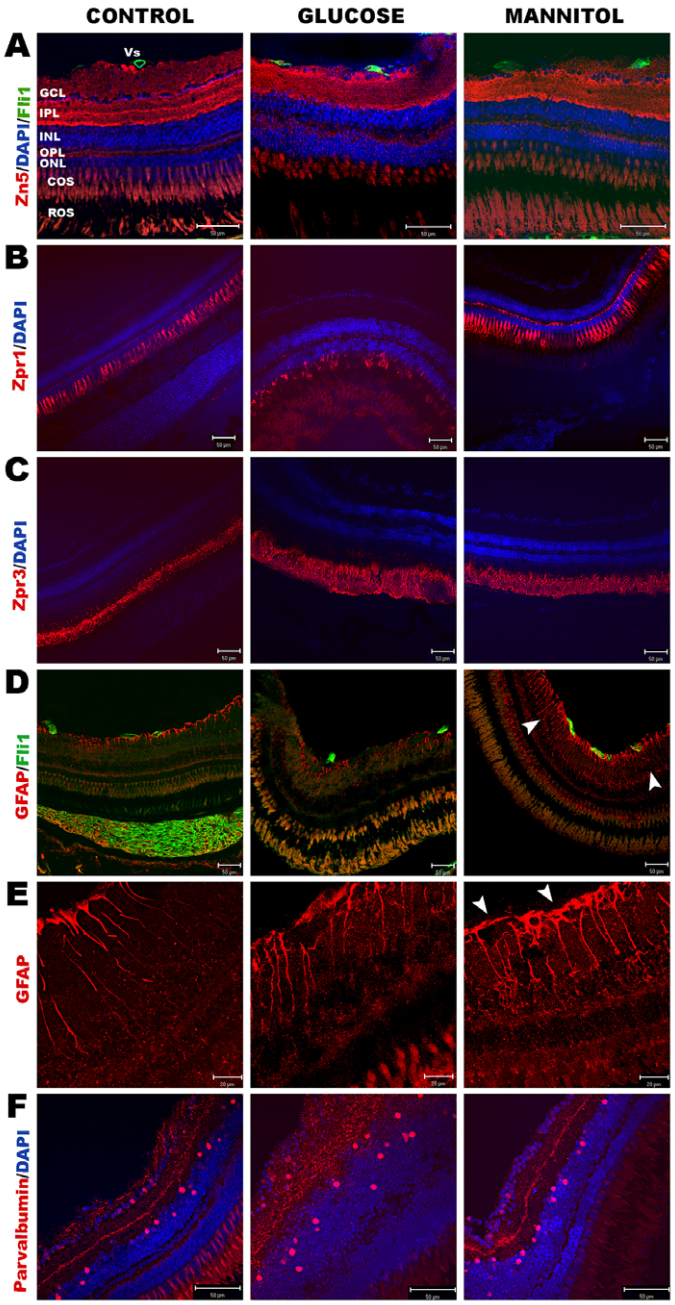

Fig. 4. Cones are affected in the hyperglycaemic zebrafish. Confocal images of immunofluorescent labelling of retinal cell types in cryosections of control (*n*=3), glucose-treated (*n*=4) and mannitol-treated (*n*=4) fish. (A) Zn5 (red) staining of ganglion cells showed no significant differences between the three experimental conditions. (B) Zpr1 (red) labelling of double cones showed weaker and discontinuous staining in all retinas from glucose-treated fish compared with control or mannitol-treated retinas. (C) Zpr3 (red) staining of rod outer segments showed no significant differences between the three experimental groups. (D,E) GFAP labelling of Müller cells (red) interacting with *Tg(Fli-1:EGFP)*-labelled retinal vessels. The retinal sections of mannitol-treated fish always showed stronger GFAP labelling than control or glucose-treated retinal sections, denoting glial activation (arrowheads). The mass of green cells in the control outer retina corresponds to choroidal vessels that have become displaced in the other retinas. (F) Parvalbumin labelling (red) of a subpopulation of inner retinal amacrine cells indicates no significant differences among the control, glucose and mannitol retinas. Variations in the thickness of the layers/staining arose from differences in the sectioning angle, and weak signals in the COS/ROS in panels A, D and F are because of autofluorescence of the photoreceptors and/or non-specific antibody binding. DAPI (blue) nuclear staining is shown in A, B, C and F. Bars, 50 µm (A-D,F); 20 µm (E). GCL, ganglion cell layer; IPL, inner plexiform layer; OPL, outer plexiform layer; INL, inner nuclear layer; ONL, outer nuclear layer; COS, cone outer segments; ROS, rod outer segments; Vs, vessel.

morphological perturbations of rods, but these changes are significantly milder than the prevalent cone photoreceptor degeneration. However, studies in rodents would not easily identify cone defects owing to the rod-dominant retinas of these nocturnal animals.

Is disrupted cone physiology likely to occur in diabetics? ERG analysis of non-retinopathic diabetics reveals significant reductions in the b-wave amplitude of S-cones (Greenstein et al., 2000; Gardner et al., 2002; Mortlock et al., 2005; Simo et al., 2006). Indeed, an abnormal S-cone ERG is proposed to predict the development of PDR in asymptomatic patients (Yamamoto et al., 1996). Our data suggest that, in diabetics, attenuated ERG responses result from perturbed cone photoreceptor morphology followed by cone degeneration. It is intriguing that, compared with rods, zebrafish cones have an enhanced susceptibility to hyperglycaemia-induced neurodegeneration. We can only speculate on the mechanism, but this finding is recapitulated in humans. Kurtenbach et al. report that, in humans exposed to hyperglycaemia, cone metabolism is significantly enhanced compared with rod metabolism (Kurtenbach et al., 2006).

There is debate about whether the development of neuropathology and microangiopathy in DR are independent events (Simo et al., 2006; Hernandez and Simo, 2007). Our data demonstrate that the cone dysfunction induced by hyperglycaemia develops independent of the early vascular pathologies and GCL apoptosis induced by hyperosmolarity. As mannitol permeabilises the brain/retinal-blood barriers, it has been administered clinically to release intracranial pressure after head trauma, to relieve intraocular pressure in glaucoma, and to facilitate the delivery of drugs to the central nervous system (Lam et al., 2002; Jin et al., 2007; Engelhard et al., 2008). Our results demonstrating neuronal apoptosis in the GCL suggest cautious long-term, clinical use of mannitol. By contrast, hyperglycaemia disrupts the blood-retinal barrier, thickens the retinal vessel basement membrane, and induces cone degeneration (Table 1). Thus, blood-retinal barrier perturbation and elevated VEGF expression are not sufficient to induce cone neurodegeneration.

The pro-angiogenic VEGF is significantly elevated in NPDR where it is thought to induce vascular leakage (Sone et al., 1996; Sone et al., 1997; Brownlee, 2001; Simo et al., 2006). Anti-VEGF treatments targeting vascular pathology are in clinical trials for DR (Campochiaro, 2007). However, VEGF also controls neuronal function. In one report, diminishment of VEGF expression in the retina resulted in photoreceptor degeneration (Saint-Geniez et al., 2008). In another report, overexpression of VEGF in the retina resulted in photoreceptor degeneration (van Eeden et al., 2006).

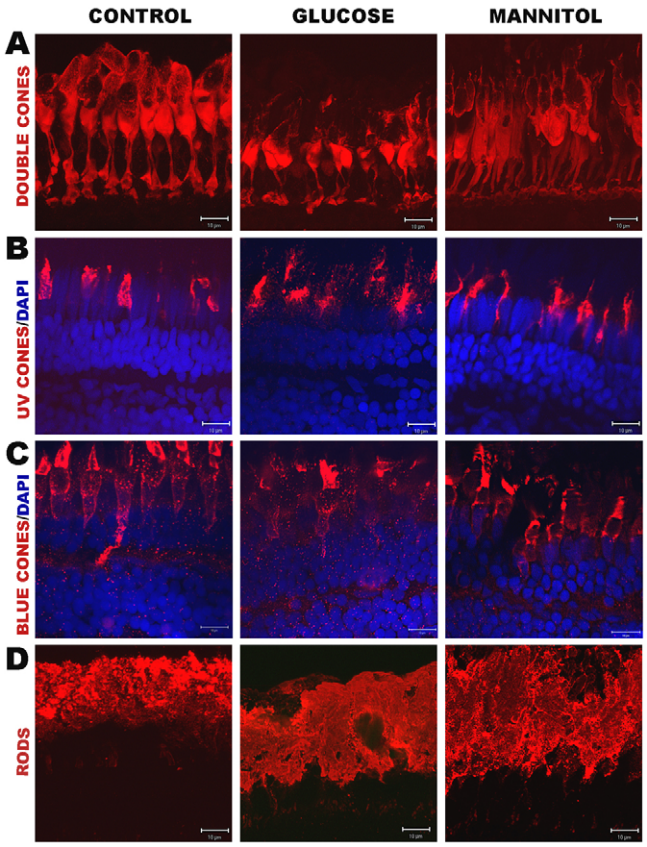

Fig. 5. All cone types are affected in the retinas of glucose-treated fish. High magnification confocal images of the different photoreceptor types in control (*n*=3), glucose-treated (*n*=4) and mannitol-treated (*n*=4) fish. (A) Zpr1 labelling in glucose-treated fish shows stubby and irregularly stained double cones compared with mannitol-treated and control fish. (B,C) UV and blue cones labelled with monoclonal antibodies against zebrafish UV and blue opsin, respectively, are less affected, but exhibit weaker and more irregular staining in glucose-treated retinas compared with mannitol-treated or control fish. (D) Labelling of the rod outer segments showed no major differences among the three treatment groups. Variations in the thickness of the layers/staining arose from differences in the sectioning angle. DAPI (blue) nuclear staining is shown in B and C. Bars, 10 µm. (Additional immunohistochemistry images are shown in supplementary material Fig. S2.)

Thus, new therapies for DR may have to move away from VEGF with the goal of inhibiting vascular pathologies and providing neuroprotection for the photoreceptors.

DR is a complex disorder. Our understanding of DR has increased with established in vivo and in vitro models. However, alternative animal models that reveal novel aspects of DR pathophysiology and/or that facilitate discovery of improved therapeutic intervention are welcome. An advantage of the zebrafish DR model is the ease of assessing the well-characterised microvascular and neuronal networks in the retina (Alvarez et al., 2007; Cao et al., 2008; Kitambi et al., 2009). In addition, zebrafish are suited to targeted and random pharmacological screens which may uncover novel drugs that prevent vascular pathology or that protect from neuropathology (Chan et al., 2002; Bayliss et al., 2006; Hong, 2009; Kitambi et al., 2009; Mandrekar and Thakur, 2009).

METHODS

Glucose and mannitol treatments

Tg(fli1:EGFP) zebrafish were maintained according to standard procedures on a 14-hour light/10-hour dark cycle at 28°C (Westerfield, 2000). Three independent glucose treatments were performed on a total of 33 1-year-old zebrafish (control, *n*=5; glucose, *n*=28) and 125 2-year-old zebrafish (control, *n*=29; mannitol, *n*=32; glucose, *n*=64), essentially following the protocol of Gleeson et al. (Gleeson et al., 2007). Briefly, groups of five fish per 2-litre tank were subjected to 24-hour treatments with 2% glucose or 2% mannitol (~110 mM), followed by 24 hours in freshly prepared system water, for 30 days. Control fish were kept in the system water for the entire 30-day treatment. To avoid bacterial contamination, system water was prepared using distilled water and adjusted to approximately pH 7 and a conductivity of ~1000 µS. After every 24 hours of glucose/mannitol treatment, fish were rinsed in distilled water for 5-10 seconds before transfer to a clean tank of system water. Fish were fed once a week and monitored twice a day. Distressed animals (~20%) were euthanised immediately. All experiments were carried out under ethical approval granted by the UCD animal research ethics committee and subject to a licence from the Irish Department of Health and Children.

Retinal dissection and imaging of retinal vessels

Adult zebrafish were euthanised with benzocaine and rinsed in PBS. Eyes were enucleated and fixed in 4% PFA at 4°C overnight. Retinas were dissected and prepared for imaging of the vasculature, as described previously (Alvarez et al., 2007). The retinas of 1-year-old fish were stored in methanol before analysis, which reduced vessel thickness by ~25%. Vessels were visualised using bright-field, epifluorescence, and confocal microscopy (Zeiss Lumar V12 stereo microscope; Olympus SZX16 stereo zoom microscope; Zeiss UV510 META LSM confocal microscopy system).

Reverse transcription PCR

Total RNA was isolated from pools of at least 2-4 control, glucose and mannitol retinas using the RNeasy kit (Qiagen). For each condition, RNA extraction was conducted on two separate pools of retinas (from two independent treatments) to have duplicates of the data. cDNA was synthesised by reverse transcription using a Superscript III kit (Invitrogen). Standard PCR was carried out using 1 U of Taq-DNA polymerase (Invitrogen) per reaction. PCR products were visualized on 1% agarose/ethidium bromide gels. The primer sequences and product sizes for each amplicon analysed are listed in supplementary Table S1.

Immunohistochemistry

Eyes were fixed in 4% PFA overnight and cryoprotected with 15% sucrose in PBS. Eyes were subsequently embedded in Tissue-Tek (Sakura Finetek Europe) and kept at −80°C before 10-µm cryosections were cut. Cryosections were dried at room temperature for 30 minutes, gradually dehydrated in methanol and then re-hydrated in PBS. Sections were permeabilised with 0.1% Tween in PBS for 10 minutes, treated with blocking solution (PBS, 0.1% Tween, 1% BSA, 5% goat serum) at room temperature, followed by incubation of the primary antibody (diluted 1:50 to 1:100 in blocking solution) at 4°C overnight.

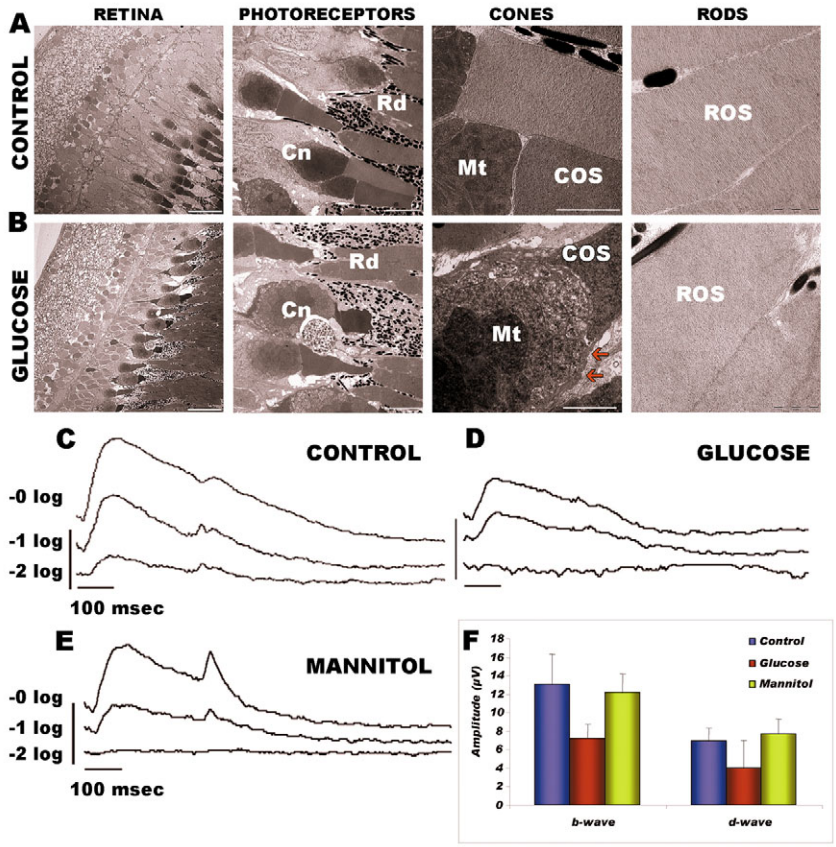

Fig. 6. Cone degeneration in glucose-treated fish correlates with deficient ERG. (A,B) A series of representative TEM images of photoreceptors in control fish with normal ERGs (A) and glucose-treated fish displaying abnormal ERGs (B). The photoreceptor layer appears to be undergoing a neurodegenerative process in glucose-treated fish. Cones are clearly shorter and dysmorphic, and appear much more affected than rods. Tissue vacuolations with large intercellular spaces and plasma membrane discontinuities (red arrows) in the cone photoreceptors of glucose-treated fish suggest necrotic cell death. The mitochondria (Mt) from the cones of glucose-treated fish are deteriorated and disordered. The cone outer segments (COS) in glucose-treated fish are disorganised and, in most cases, no laminar stacked structures can be distinguished at the higher magnification. The rod outer segments (ROS) seem mildly affected by glucose and laminar structures are easily distinguished. Bars, 20 μm (A,B; far left column), 5 μm (second column from the left), 2 μm (A,B; second column from the right); 1 μm (A,B; far right column). Cn, cone; Rd, rod; Mt, mitochondria; COS, cone outer segment; ROS, rod outer segment. (C-E) Representative ERGs of control (C), glucose-treated (D) and mannitol-treated (E) fish in response to a 300 millisecond flash of light. Full-field flash intensities at –2 log, –1 log and 0 log are shown. The vertical scale bar is 10 microvolts and the horizontal scale bar is 100 milliseconds. Each tracing is the average of 5-10 signals. (F) Graph showing, within each treatment group, the average b- and d-wave amplitudes from photopic ERGs at the maximum flash intensity (–0 log).

The primary antibody was washed three times, for 5 minutes each, in 5% goat serum-PBS and incubated in the same solution for 1 hour at room temperature with Cy2- or Cy3-labeled anti-mouse or anti-rabbit antibodies, diluted 1:200 in blocking solution (Jackson Labs). Sections were photo-protected with Vectashield (Vector), coverslipped and sealed prior to confocal microscopy. The following primary antibodies used were: (1) zn5, for retinal ganglion cells; (2) zpr1, for double cone photoreceptors; (3) anti-UV opsin, for UV cones; (4) anti-blue opsin, for blue cones; (5) zpr3, for rod outer segments; (6) GFAP, for Müller cells; and (7) parvalbumin, for amacrine cells.

Apoptosis assay (TUNEL)

TUNEL was carried out on 10-μm cryosections following the manufacturer's instructions (In Situ Cell Death Detection kit, Roche). Briefly, sections were treated with proteinase K (2 μg/ml) and dehydrated with a mixture of 70% ethanol/30% acetic acid. Sections were re-fixed in 4% PFA for 5 minutes at 4°C, and 50 μl of labelling mix and 50 μl of TUNEL mix were added to each section. Sections were covered with coverslips and incubated in the dark at 37°C overnight. After washing in PBS, sections were photo-protected with Vectashield (Vector), coverslipped and sealed prior to confocal microscopy.

Table 1. Diabetic retinopathy hallmarks: a comparison of the microangiopathic and neurodegenerative phenotypes observed in glucose- and mannitol-treated zebrafish and human diabetic retinopathy

DR hallmarks		Human diabetes	Glucose-treated zebrafish	Mannitol-treated zebrafish
Vascular	Opening of retinal blood barrier junctions	Confirmed*	Confirmed	Confirmed
	Increased VEGF expression	Confirmed	Confirmed	Confirmed
	Dilated retinal vessels	Confirmed	Confirmed	X
	Basement membrane thickening in retinal capillaries	Confirmed*	Confirmed	X
	Loss of retinal pericytes	Confirmed*	X	X
	Retinal neovascularisation	Confirmed	X	X
	Glial activation	Confirmed*	X	Confirmed
Neuronal	Impaired photoreceptor physiology	Confirmed	Confirmed	X
	Cone morphology degeneration	?*	Confirmed	X
	Apoptosis in GCL and INL	?*	X	Confirmed

Key: X, not found; ?, not determined/controversial results; *based on post-mortem evidence.

Histology and ultrastructural analysis

Retinas for transmission electron microscopy (TEM) were prepared as described previously (Alvarez et al., 2007). Briefly, eyes were fixed in Sorensen phosphate buffer (pH 7.3) containing 4% PFA and 2.5% glutaraldehyde, then embedded in Epon resin. Semi-thin (1 μm) sections were examined under light microscopy for histological analysis, and ultra-thin sections (100 nm) were examined using a Tecnai 12 BioTwin transmission electron microscope (FEI Electron Optics) for ultrastructural investigation.

Ex-vivo electroretinograms (ERG)

ERGs were recorded from adult zebrafish eyecups. Briefly, zebrafish were euthanised in 4% 3-aminobenzoic acid methylester and the eyes enucleated. The cornea and lens were removed by microdissection. The eyecup was immediately placed onto filter paper in the recording chamber and oxygenated (95% O_2/5% CO_2). Minimal essential medium (MEM) was perfused directly into the eyecup at ~0.4 ml/minute. The recording electrode, a thick-walled glass capillary (tip diameter: 80-100 μm) containing 0.9% saline, was placed within the eyecup, not touching the retina. The reference electrode, a bleached silver/silver chloride wire, was placed underneath the filter paper. The voltage signal was amplified using a differential P55 pre-amplifier (Grass Instruments) with a bandpass of 0.1 and 100 Hz. A 50-Hz line filter was switched on in order to remove cyclical noise. The eyecup was left to equilibrate in the dark for 30 minutes to adapt to the new conditions. A 300-W tungsten light source was used for stimulus and an LED light source for background light.

The unattenuated irradiances for the background and the stimulus were 50 $\mu W/cm^2$ and 2.8×10^3 $\mu W/cm^2$, respectively. Stimulus flash duration was controlled by a mechanical shutter (Newport Corporation) and the rate was controlled by an S48 stimulator (Grass Instruments). Data were acquired using a PC with a NiDAQ 6024E board, running Windows Whole Cell Program (WinWCP, University of Strathclyde). Full-field white flashes (300 mseconds) were presented every 30 seconds to the dark-adapted eye. Following 20 minutes of light adaptation, full-field white flash (300 mseconds) presentation was carried out every 10 seconds. The data were signal averaged (5-10 signals). For all recordings, flashes attenuated by 2.0, 1.0 and 0 (unattenuated) log units were used. The amplitude of the various waves was measured as described previously (Wong et al., 2004).

Statistical analyses

P values were calculated based on a *t*-test with two samples and assuming unequal variances.

ACKNOWLEDGEMENTS

We would like to thank Professor David Hyde for providing us with anti-UV and anti-blue opsin antibodies; Beata Sapetto-Rebow for technical assistance; Dr David C. Cottell for expert technical advice on TEM; and Professor Alan Stitt, Professor Cormac Taylor, Professor Tom Gardiner, Dr Ralph Nelson and Dr Derek Brazil for valuable comments on the manuscript. This work was supported by a Health Research Board (Ireland) Postdoctoral Fellowship (to Y.A.; PD2006-32), a Science Foundation Ireland Investigator Grant (to B.N.K.; 04/IN3/B559), a Travelling Fellowship from the Company of Biologists (to A.L.R.) and a Science Foundation Ireland UREKA Site Award (to K.C.; 06/UR/B913).

COMPETING INTERESTS

The authors declare no competing financial interests.

AUTHOR CONTRIBUTIONS

Y.A. conducted and supervised the glucose/mannitol treatments; performed the retinal histology, TEM, RT-PCR, immunohistochemistry and confocal experiments and analyses; and wrote the manuscript. K.C. and N.W. conducted the glucose/mannitol treatments, and carried out the vascular patterning and immunohistochemistry experiments and analyses. A.L.R. and J.O'C. performed and/or contributed to the ERG experiments and analyses, and manuscript writing. B.N.K. conceived, designed and supervised the study; and provided major contributions in shaping and writing the manuscript.

TRANSLATIONAL IMPACT

Clinical issue

More than 2.5 million people in the world are blind as a consequence of diabetic retinopathy (DR). One of the most common clinical complications of diabetes, DR results from abnormal changes in the vascularisation of the retina, coupled to neurodegeneration. Current therapies target the advanced proliferative stage of the disease, stunting the inappropriate growth of new blood vessels, after much damage has already been done; treatment is not curative and has serious side effects. A better, potentially curative, approach might be to target the earlier non-proliferative stage of DR, and to protect the endangered retinal neurons. However, the progression of DR in its early stages is not well understood, as human data typically originate from post-mortem tissue at advanced stages, and animal models have given conflicting results. Important issues include which retinal neurons are affected in DR, when neuronal damage occurs, and whether neuronal damage depends on vascular injury.

Results

This paper suggests that zebrafish can successfully model non-proliferative DR, using a protocol in which hyperglycaemia is induced by adding glucose to tank water every other day for a month. Retinas from zebrafish subjected to this oscillating hyperglycaemia display many of the pathophysiological aspects of human DR. Vascular changes include thickening of the basal membrane, disturbance of the retinal blood barrier, and dilation of retinal capillaries. Interestingly, hyperglycaemia also induces pronounced neurodegeneration of cone photoreceptors without drastic effects on other retinal cell types, whereas treatment with mannitol, which causes hyperosmolarity but not hyperglycaemia, induces vascular changes without cone photoreceptor damage.

Implications and future directions

In this zebrafish model, hyperglycaemia induces cone receptor dysfunction, and hence neuronal damage, at early stages in DR, independently of vascular defects, and before the proliferative stage of the disease. Future work needs to confirm whether cone photoreceptors are particularly susceptible to damage by hyperglycaemia in humans and other higher mammals. Such findings would revise DR treatment strategies to include neuroprotection of cone photoreceptors in addition to inhibiting vascular pathology.

doi:10.1242/dmm.005280

SUPPLEMENTARY MATERIAL

Supplementary material for this article is available at
http://dmm.biologists.org/lookup/suppl/doi:10.1242/dmm.003772/-/DC1

Received 20 August 2009; Accepted 14 September 2009.

REFERENCES

Alvarez, Y., Cederlund, M. L., Cottell, D. C., Bill, B. R., Ekker, S. C., Torres-Vazquez, J., Weinstein, B. M., Hyde, D. R., Vihtelic, T. S. and Kennedy, B. N. (2007). Genetic determinants of hyaloid and retinal vasculature in zebrafish. *BMC Dev. Biol.* **7**, 114.

Barber, A. J., Lieth, E., Khin, S. A., Antonetti, D. A., Buchanan, A. G. and Gardner, T. W. (1998). Neural apoptosis in the retina during experimental and human diabetes. Early onset and effect of insulin. *J. Clin. Invest.* **102**, 783-791.

Bayliss, P. E., Bellavance, K. L., Whitehead, G. G., Abrams, J. M., Aegerter, S., Robbins, H. S., Cowan, D. B., Keating, M. T., O'Reilly, T., Wood, J. M. et al. (2006). Chemical modulation of receptor signaling inhibits regenerative angiogenesis in adult zebrafish. *Nat. Chem. Biol.* **2**, 265-273.

Bresnick, G. H. and Palta, M. (1987). Predicting progression to severe proliferative diabetic retinopathy. *Arch. Ophthalmol.* **105**, 810-814.

Brownlee, M. (2001). Biochemistry and molecular cell biology of diabetic complications. *Nature* **414**, 813-820.

Campochiaro, P. A. (2007). Targeted pharmacotherapy of retinal diseases with ranibizumab. *Drugs Today (Barc.)* **43**, 529-537.

Cao, R., Jensen, L. D., Soll, I., Hauptmann, G. and Cao, Y. (2008). Hypoxia-induced retinal angiogenesis in zebrafish as a model to study retinopathy. *PLoS ONE* **3**, e2748.
Carrasco, E., Hernandez, C., Miralles, A., Huguet, P., Farres, J. and Simo, R. (2007). Lower somatostatin expression is an early event in diabetic retinopathy and is associated with retinal neurodegeneration. *Diabetes Care* **30**, 2902-2908.
Carrasco, E., Hernandez, C., de Torres, I., Farres, J. and Simo, R. (2008). Lowered cortistatin expression is an early event in the human diabetic retina and is associated with apoptosis and glial activation. *Mol. Vis.* **14**, 1496-1502.
Chan, J., Bayliss, P. E., Wood, J. M. and Roberts, T. M. (2002). Dissection of angiogenic signaling in zebrafish using a chemical genetic approach. *Cancer Cell* **1**, 257-267.
Cho, N. C., Poulsen, G. L., Ver Hoeve, J. N. and Nork, T. M. (2000). Selective loss of S-cones in diabetic retinopathy. *Arch. Ophthalmol.* **118**, 1393-1400.
Daley, M. L., Watzke, R. C. and Riddle, M. C. (1987). Early loss of blue-sensitive color vision in patients with type I diabetes. *Diabetes Care* **10**, 777-781.
Engelhard, K., Muller-Forell, W. and Werner, C. (2008). [Therapy of head trauma]. *Anaesthesist.* **57**, 1219-1231.
Feit-Leichman, R. A., Kinouchi, R., Takeda, M., Fan, Z., Mohr, S., Kern, T. S. and Chen D. F. (2005). Vascular damage in a mouse model of diabetic retinopathy, relation to neuronal and glial changes. *Invest. Ophthalmol Vis. Sci.* **46**, 4281-4287.
Frank, R. N. (2004). Diabetic retinopathy. *N. Engl. J. Med.* **350**, 48-58.
Frank, R. N. (2009). Treating diabetic retinopathy by inhibiting growth factor pathways. *Curr. Opin. Investig. Drugs* **10**, 327-335.
Fraser, R. B., Waite, S. L., Wood, K. A. and Martin, K. L. (2007). Impact of hyperglycemia on early embryo development and embryopathy, in vitro experiments using a mouse model. *Hum. Reprod.* **22**, 3059-3068.
Gardner, T. W., Antonetti, D. A., Barber, A. J., LaNoue, K. F. and Levison, S. W. (2002). Diabetic retinopathy, more than meets the eye. *Surv. Ophthalmol.* **47 Suppl. 2**, S253-S262.
Garner, A. (1970). Pathology of diabetic retinopathy. *Br. Med. Bull.* **26**, 137-142.
Gleeson, M., Connaughton, V. and Arneson, L. S. (2007). Induction of hyperglycaemia in zebrafish (Danio rerio) leads to morphological changes in the retina. *Acta. Diabetol.* **44**, 157-163.
Greenstein, V. C., Holopigian, K., Hood, D. C., Seiple, W. and Carr, R. E. (2000). The nature and extent of retinal dysfunction associated with diabetic macular edema. *Invest. Ophthalmol. Vis. Sci.* **41**, 3643-3654.
Haselton, F. R., Dworska, E. J. and Hoffman, L. H. (1998). Glucose-induced increase in paracellular permeability and disruption of beta-receptor signaling in retinal endothelium. *Invest. Ophthalmol. Vis. Sci.* **39**, 1676-1684.
Hernandez, C. and Simo, R. (2007). Strategies for blocking angiogenesis in diabetic retinopathy, from basic science to clinical practice. *Expert. Opin. Investig. Drugs* **16**, 1209-1226.
Hong, C. C. (2009). Large-scale small-molecule screen using zebrafish embryos. *Methods Mol. Biol.* **486**, 43-55.
Ihnat, M. A., Thorpe, J. E., Kamat, C. D., Szabo, C., Green, D. E., Warnke, L. A., Lacza, Z., Cselenyak, A., Ross, K., Shakir, S. et al. (2007). Reactive oxygen species mediate a cellular 'memory' of high glucose stress signalling. *Diabetologia* **50**, 1523-1531.
Jin, X., Xue, A., Zhao, Y., Qin, Q., Dong, X. D. and Qu, J. (2007). Efficacy and safety of intravenous injection of lidocaine in the treatment of acute primary angle-closure glaucoma, a pilot study. *Graefes Arch. Clin. Exp. Ophthalmol.* **245**, 1611-1616.
Juen, S. and Kieselbach, G. F. (1990). Electrophysiological changes in juvenile diabetics without retinopathy. *Arch. Ophthalmol.* **108**, 372-375.
Kinkel, M. D. and Prince, V. E. (2009). On the diabetic menu, zebrafish as a model for pancreas development and function. *BioEssays* **31**, 139-152.
Kitambi, S. S., McCulloch, K. J., Peterson, R. T. and Malicki, J. J. (2009). Small molecule screen for compounds that affect vascular development in the zebrafish retina. *Mech. Dev.* **126**, 464-477.
Klein, R., Klein, B. E., Moss, S. E., Davis, M. D. and DeMets, D. L. (1984). The Wisconsin epidemiologic study of diabetic retinopathy. III. Prevalence and risk of diabetic retinopathy when age at diagnosis is 30 or more years. *Arch. Ophthalmol.* **102**, 527-532.
Kurtenbach, A., Mayser, H. M., Jagle, H., Fritsche, A. and Zrenner, E. (2006). Hyperoxia, hyperglycemia, and photoreceptor sensitivity in normal and diabetic subjects. *Vis. Neurosci.* **23**, 651-661.
Lam, D. S., Chua, J. K., Tham, C. C. and Lai, J. S. (2002). Efficacy and safety of immediate anterior chamber paracentesis in the treatment of acute primary angle-closure glaucoma, a pilot study. *Ophthalmology* **109**, 64-70.
Li, Q., Zemel, E., Miller, B. and Perlman, I. (2002). Early retinal damage in experimental diabetes, electroretinographical and morphological observations. *Exp. Eye Res.* **74**, 615-625.
Makino, S., Kunimoto, K., Muraoka, Y., Mizushima, Y., Katagiri, K. and Tochino, Y. (1980). Breeding of a non-obese, diabetic strain of mice. *Jikken Dobutsu* **29**, 1-13.
Mandal, A. K., Ping, T., Caldwell, S. J., Bagnell, R. and Hiebert, L. M. (2006). Electron microscopic analysis of glucose-induced endothelial damage in primary culture, possible mechanism and prevention. *Histol. Histopathol.* **21**, 941-950.
Mandrekar, N. and Thakur, N. L. (2009). Significance of the zebrafish model in the discovery of bioactive molecules from nature. *Biotechnol. Lett.* **31**, 171-179.
Martin, P. M., Roon, P., Van Ells, T. K., Ganapathy, V. and Smith, S. B. (2004). Death of retinal neurons in streptozotocin-induced diabetic mice. *Invest Ophthalmol. Vis. Sci.* **45**, 3330-3336.
Morello, C. M. (2007). Etiology and natural history of diabetic retinopathy, an overview. *Am. J. Health Syst. Pharm.* **64**, S3-S7.
Mortlock, K. E., Chiti, Z., Drasdo, N., Owens D. R. and North, R. V. (2005). Silent substitution S-cone electroretinogram in subjects with diabetes mellitus. *Ophthalmic Physiol. Opt.* **25**, 392-399.
Nakhooda, A. F., Like, A. A., Chappel, C. I., Murray, F. T. and Marliss, E. B. (1977). The spontaneously diabetic Wistar rat. Metabolic and morphologic studies. *Diabetes* **26**, 100-112.
Pampfer, S., Cordi, S., Vanderheyden, I., Van Der Smissen, P., Courtoy, P. J., Van Cauwenberge, A., Alexandre, H., Donnay, I. and De Hertogh, R. (2001). Expression and role of Bcl-2 in rat blastocysts exposed to high D-glucose. *Diabetes* **50**, 143-149.
Parisi, V. and Uccioli, L. (2001). Visual electrophysiological responses in persons with type 1 diabetes. *Diabetes Metab. Res. Rev.* **17**, 12-18.
Park, S. H., Park, J. W., Park, S. J., Kim, K. Y., Chung, J. W., Chun, M. H. and Oh, S. J. (2003). Apoptotic death of photoreceptors in the streptozotocin-induced diabetic rat retina. *Diabetologia* **46**, 1260-1268.
Portha, B., Giroix, M. H., Serradas, P., Gangnerau, M. N., Movassat, J., Rajas, F., Bailbe, D., Plachot, C., Mithieux, G. and Marie, J. C. (2001). beta-cell function and viability in the spontaneously diabetic GK rat, information from the GK/Par colony. *Diabetes* **50 Suppl. 1**, S89-S93.
Rees D. A. and Alcolado, J. C. (2005). Animal models of diabetes mellitus. *Diabet Med.* **22**, 359-370.
Ruberte, J., Ayuso, E., Navarro, M., Carretero, A., Nacher, V., Haurigot, V., George, M., Llombart, C., Casellas, A., Costa, C. et al. (2004). Increased ocular levels of IGF-1 in transgenic mice lead to diabetes-like eye disease. *J. Clin. Invest.* **113**, 1149-1157.
Saint-Geniez, M., Maharaj, A. S., Walshe, T. E., Tucker, B. A., Sekiyama, E., Kurihara, T., Darland, D. C., Young, M. J. and D'Amore, P. A. (2008). Endogenous VEGF is required for visual function, evidence for a survival role on muller cells and photoreceptors. *PLoS ONE* **3**, e3554.
Shen, W. Y., Lai, Y. K., Lai, C. M., Binz, N., Beazley, L. D., Dunlop, S. A. and Rakoczy, P. E. (2006). Pathological heterogeneity of vasoproliferative retinopathy in transgenic mice overexpressing vascular endothelial growth factor in photoreceptors. *Adv. Exp. Med. Biol.* **572**, 187-193.
Simo, R. and Hernandez, C. (2008). Intravitreous anti-VEGF for diabetic retinopathy, hopes and fears for a new therapeutic strategy. *Diabetologia* **51**, 1574-1580.
Simo, R., Carrasco, E., Garcia-Ramirez, M. and Hernandez, C. (2006). Angiogenic and antiangiogenic factors in proliferative diabetic retinopathy. *Curr. Diabetes Rev.* **2**, 71-98.
Sone, H., Okuda, Y., Kawakami, Y., Hanatani, M., Suzuki, H., Kozawa, T., Honmura, S. and Yamashita, K. (1996). Vascular endothelial growth factor level in aqueous humor of diabetic patients with rubeotic glaucoma is markedly elevated. *Diabetes Care* **19**, 1306-1307.
Sone, H., Kawakami, Y., Okuda, Y., Sekine, Y., Honmura, S., Matsuo, K., Segawa, T., Suzuki, H. and Yamashita, K. (1997). Ocular vascular endothelial growth factor levels in diabetic rats are elevated before observable retinal proliferative changes. *Diabetologia* **40**, 726-730.
van Eeden, P. E., Tee, L. B., Lukehurst, S., Lai, C. M., Rakoczy, E. P., Beazley, L. D. and Dunlop, S. A. (2006). Early vascular and neuronal changes in a VEGF transgenic mouse model of retinal neovascularization. *Invest. Ophthalmol. Vis. Sci.* **47**, 4638-4645.
Vinores, S. A., Sen, H. and Campochiaro, P. A. (1992). An adenosine agonist and prostaglandin E1 cause breakdown of the blood-retinal barrier by opening tight junctions between vascular endothelial cells. *Invest. Ophthalmol. Vis. Sci.* **33**, 1870-1878.
Westerfield, M. (2000). The zebrafish book. A guide for the laboratory use of zebrafish (Danio rerio). 4th ed, in (Univ. of Oregon Press E ed).
Wilkinson-Berka, J. L. and Miller, A. G. (2008). Update on the treatment of diabetic retinopathy. *ScientificWorldJournal* **8**, 98-120.
Wolter, J. R. (1961). Diabetic retinopathy. *Am. J. Ophthalmol.* **51**, 1123-1141.
Wong, K. Y., Gray, J., Hayward, C. J., Adolph, A. R. and Dowling, J. E. (2004). Glutamatergic mechanisms in the outer retina of larval zebrafish, analysis of electroretinogram b- and d-waves using a novel preparation. *Zebrafish* **1**, 121-131.
Wong, T. Y., Klein, R., Islam, F. M., Cotch, M. F., Folsom, A. R., Klein, B. E., Sharrett, A. R. and Shea, S. (2006). Diabetic retinopathy in a multi-ethnic cohort in the United States. *Am. J. Ophthalmol.* **141**, 446-455.
Yamamoto, S., Kamiyama, M., Nitta, K., Yamada, T. and Hayasaka, S. (1996). Selective reduction of the S cone electroretinogram in diabetes. *Br. J. Ophthalmol.* **80**, 973-975.
Zeng, X. X., Ng, Y. K. and Ling, E. A. (2000). Neuronal and microglial response in the retina of streptozotocin-induced diabetic rats. *Vis. Neurosci.* **17**, 463-471.